A study of the charge and potential distribution at the semiconductor/electrolyte interface for the condition of degeneracy

Heinz Gerischer and Robert McIntyre

Citation: The Journal of Chemical Physics **83**, 1363 (1985); doi: 10.1063/1.449453
View online: http://dx.doi.org/10.1063/1.449453
View Table of Contents: http://scitation.aip.org/content/aip/journal/jcp/83/3?ver=pdfcov
Published by the AIP Publishing

A study of the charge and potential distribution at the semiconductor/electrolyte interface for the condition of degeneracy

Heinz Gerischer and Robert McIntyre
Fritz-Haber-Institut der Max-Planck-Gesellschaft, Faradayweg 4–6, D 1000 Berlin 33, West Germany

(Received 12 February 1985; accepted 22 April 1985)

We have calculated the differential surface capacitance for two different semiconductors $MoSe_2(0001)$ and $WSe_2(0001)$, as a function of applied potential, for the condition of degeneracy. The calculated curves are compared with the experimentally measured capacitance for the systems, $MoSe_2(0001)$ in propylene carbonate containing 0.1 M $LiClO_4$, for a range of crystal conductivities, and $WSe_2(0001)$ in acetonitrile containing 0.2 M $(C_3H_7)_4N\,BF_4$. As expected the experimental values are significantly lower than the calculated values, since the measured capacitance is the total capacitance for the system which is described by the surface capacitance of the semiconductor in series with the Helmholtz capacitance. Calculations based on this model, using the data for the Helmholtz capacitance for a mercury electrode in the same electrolyte, are shown to be in good agreement with the measured values. The results are discussed with particular reference to the screening distance for the semiconductor surface charge in the degenerate region.

I. INTRODUCTION

For an n-type semiconductor, at potentials giving rise to a depletion layer, the equation which describes the charge as a function of potential is very well known.[1–4] The derivative of this equation approximates to the familiar Mott–Schottky relationship for the differential capacitance in the depletion layer region. The experimental verification of the above relationship is the basis for determination of flat band potentials and donor concentration values which are generally accepted in semiconductor electrochemistry.

The derivation of the above equations assumes that the position of the Fermi level (E_F) at the semiconductor surface satisfies the condition

$$(E_V + 3kT) \leqslant E_F \leqslant (E_C - 3kT), \tag{1}$$

where E_V is the energy of the valence band maximum and E_C is the energy of the conduction band minimum. In this case the free carriers in the whole space charge region obey Boltzmann statistics. If, however, the above inequality does not hold (e.g., as the Fermi level approaches the conduction band minimum) the concentration of free carriers have to be calculated using the Fermi–Dirac distribution function.[3,4] This case is known as degeneracy of the free carriers at the surface.

To date, the authors know of only one rather early attempt to compare theory with experiment for the condition of degeneracy. Dewald[5] measured the differential capacitance for the zinc oxide/aqueous electrolyte system. However, the data do not extend far enough into the degenerate region to be comparable with the theory. The difficulty associated with the measurement of meaningful capacitance data in the degenerate region is being able to avoid any appreciable faradaic processes. For example, hydrogen evolution and/or reduction of the ZnO cannot be avoided in aqueous solution, for the condition of extreme degeneracy in such an experiment. These processes would preclude the measurement of accurate capacitance data.

In this work we have studied metal dichalcogenide semiconductor electrodes in aprotic electrolyte systems. We have found that these systems are perfectly polarizable to potentials in excess of 2.0 V negative of flat band, and as such, are ideal candidates for the experimental determination of differential capacitance under the conditions of extreme degeneracy.

A. Differential capacitance equations for the condition of degeneracy

A one-dimensional semi-infinite model for the semiconductor crystal is adopted. The counter charge is treated as lying outside the semiconductor, but immediately adjacent to the surface at ($x = 0$). The electric field in the semiconductor at the surface is obtained by integrating Poisson's equation from the neutral bulk to the surface. First, however, it is necessary to obtain an explicit expression for the charge density (ρ) as a function of potential. For an n-type semiconductor the charge density can be considered to be made up of mobile electrons and immobile ionized donors. For the condition of degeneracy we can assume that the contribution of the ionized donors, to the total space charge, is negligible in comparison with the concentration of conduction band electrons. At any point in the crystal the concentration of conduction band electrons (n) is given by[6]

$$n = \int_{E_C}^{\infty} D_C(E) f(E) dE. \tag{2}$$

We approximate the density of states function,

$$D_C(E) = 4\pi(2m^*/h^2)^{3/2}(E - E_C)^{1/2}, \tag{3}$$

where m^* is the effective mass of an electron at the bottom of the conduction band. The Fermi–Dirac distribution function $f(E)$ is given by

$$f(E) = [1 + \exp(E - E_F)/kT]^{-1}. \tag{4}$$

Thus substituting Eqs. (3) and (4) into Eq. (2) gives

 0021-9606/85/151363-08$02.10

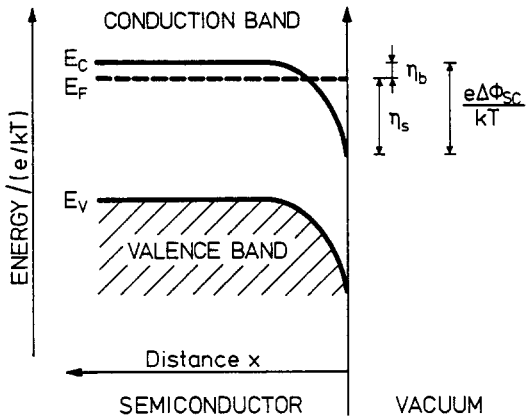

FIG. 1. A one-dimensional semi-infinite model for the potential distribution at the semiconductor/vacuum interface for the condition of degeneracy, where $\eta_b = [(E_F - E_C)/kT]_b$, $\eta_s = [(E_F - E_C)/kT]_s$, and $(\eta_s - \eta_b) = e\Delta\phi_{SC}/kT$.

$$n = 4\pi(2m^*kT/h^2)^{3/2} \times \int_{E_C}^{\infty} \frac{[(E-E_C)/kT]^{1/2}}{1+\exp[(E-E_F)/kT]}\, dE/kT. \quad (5)$$

Introducing $y = (E - E_C)/kT$; $\eta = (E_F - E_C)/kT$; $A = 4\pi(2m^*kT/h^2)^{3/2}$ and changing the variables, n can now be written in the form

$$n = AF_{1/2}(\eta), \quad (6)$$

where the function $F_j(\eta)$ (evaluated for $j = 1/2$ and $j = 3/2$ by McDougall and Stoner[7]) is defined as

$$F_j(\eta) = \int_0^{\infty} \frac{y^j dy}{1+\exp(y-\eta)}. \quad (7)$$

η is a dimensionless measure of the local potential in the semiconductor (Φ). Since the position of the band edge E_C varies with distance from the surface (x), see Fig. 1, where $E_C(x) = {}_bE_C - e\varphi(x)$; then for our one-dimensional model the Poisson equation can be written

$$\frac{d^2\eta}{dx^2} = -\frac{e}{\epsilon\epsilon_0 kT}\rho(x), \quad (8)$$

where $\rho(x) = -en(x)$. Therefore Eq. (8) becomes

$$\eta_2 = BF_{1/2}(\eta[x]), \quad (9)$$

where $B = Ae^2/\epsilon\epsilon_0 kT$ and $\eta_2 = d^2\eta/dx^2$. Equation (9) can now be written as

$$\frac{d}{dx}(\eta_1)^2 = 2B\cdot\eta_1\cdot F_{1/2}(\eta[x]), \quad (10)$$

where $\eta_1 = d\eta/dx$. Integration between the limits $x = 0$ and $x = -\infty$,

$$(\eta_1)^2|_{-\infty}^{0} = \int_{-\infty}^{0} 2B\cdot\eta_1\cdot F_{1/2}(\eta[x])\cdot dx \quad (11)$$

which can be rewritten as

$$(\eta_1)^2|_{x=0} = 2B\int_{\eta_b}^{\eta_s} F_{1/2}(\eta)\cdot d\eta, \quad (12)$$

where η_s and η_b are the surface and bulk values of η. Which gives

$$(\eta_1)^2|_{x=0} = \tfrac{4}{3}B\int_{\eta_b}^{\eta_s} \frac{d}{d\eta}\cdot F_{3/2}(\eta)\cdot d\eta. \quad (13)$$

Therefore, the dimensionless equivalent of the electric field $d\eta/dx = \eta$ becomes

$$\eta_1 = \left.\frac{d\eta}{dx}\right|_{x=0} = \{\tfrac{4}{3}B[F_{3/2}(\eta_s) - F_{3/2}(\eta_b)]\}^{1/2}. \quad (14)$$

From Gauss's law the electric field at the surface can be related to the charge in the semiconductor (Q_{SC}).

$$Q_{SC} = \epsilon\epsilon_0 \left.\frac{d\eta}{dx}\right|_{x=0} = \left\{\frac{4}{3}\frac{\epsilon\epsilon_0 e^2}{kT}A\cdot[F_{3/2}(\eta_s) - F_{3/2}(\eta_b)]\right\}^{1/2}, \quad (15)$$

where η gives the potential in units of kT/e,

$$Q_{SC} = \left\{\frac{16}{3}\frac{\epsilon\epsilon_0 e^2\pi(2m^*kT/h^2)^{3/2}}{kT} \cdot[F_{3/2}(\eta_s) - F_{3/2}(\eta_b)]\right\}^{1/2}. \quad (16)$$

For large positive values of η the function $F_j(\eta)$ takes the limiting form

$$\lim_{\eta\to\infty} F_j(\eta) = (j+1)^{-1}\eta^{j+1}. \quad (17)$$

For $\eta = 20$ the limiting form gives $F_{3/2}(\eta)$ to better than 1.6% with the accuracy of approximation increasing with increasing values of η.[7] Therefore, for large values of $(\eta_s - \eta_b)$,

$$Q_{SC} = \left[\frac{32\epsilon\epsilon_0 e^2\pi(2m^*kT/h^2)^{3/2}}{15\,kT}\right]^{1/2}(\eta_s - \eta_b)^{5/4}. \quad (18)$$

Differentiation of Eqs. (16) and (18), with respect to the surface potential of the semiconductor, gives the differential surface capacitance in the respective potential range described by

$$C_{SC} = \frac{e}{kT}\frac{dQ_{SC}}{d(\eta_s - \eta_b)}. \quad (19)$$

II. EXPERIMENTAL

N-type $MoSe_2(0001)$ and n-$WSe_2(0001)$ were prepared in the Fritz-Haber-Institut by gas phase transportation.[8] The solid state and chemical properties of layered compounds in general have been extensively reviewed.[9–15] The electrode preparation and surface classification have been described elsewhere.[16] Purification of the acetonitrile (ACN) and propylene carbonate (PC) is a lengthy procedure which has been described in detail previously.[17] The electrolytes; tetrapropylammonium tetrafluoroborate (Fluka) was recrystallized twice from H_2O and dried under vacuum for 24 h at 65 °C, lithium perchlorate (Fluka) was recrystallized twice from H_2O, dried under vacuum at 80 °C and then sealed in a glass ampoule prior to transfer to a dry atmosphere. All solutions were deoxygenated with Argon (Linde 6.0), which was first passed through an oxysorb column (Messer–Griesheim GmbH), for 30 min. The reference electrode in both cases was $Ag/AgNO_3(10^{-3}$ M).[17]

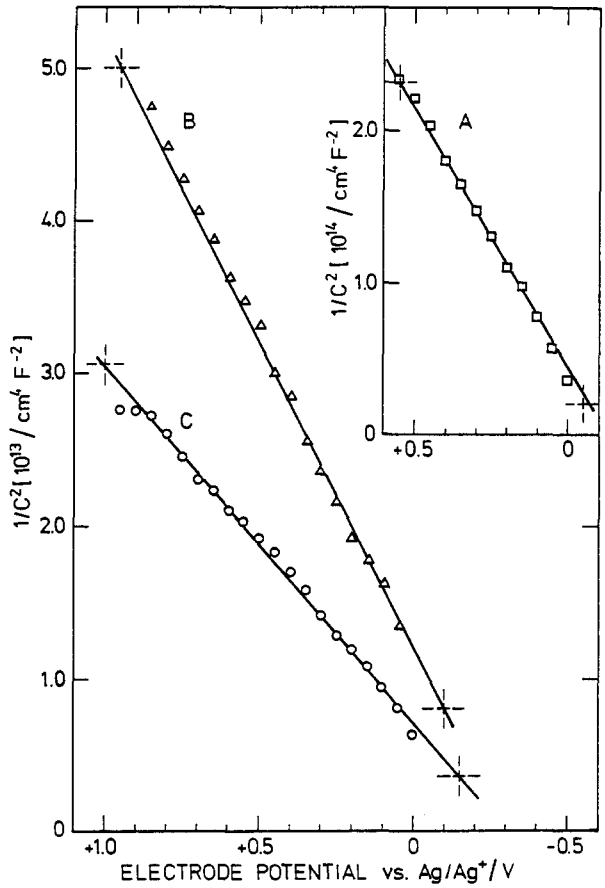

FIG. 2. Mott–Schottky plots for n-$MoSe_2$(0001), crystals A, B, and C, in propylene carbonate containing 0.1 M $LiClO_4$.

The capacitance measurements were carried out point by point as a function of applied potential. Using a lock-in amplifier (PAR model HR-8), with an internal oscillator, an ac signal with 10 mV rms was used to modulate the applied dc potential. Assuming a simple RC series network, the capacitance was calculated from the real and imaginary components of the voltage output by applying Eq. (20):

$$C_{\text{exp}} = \frac{I(1+(R/I)^2)}{v \cdot R_m \cdot \omega}, \tag{20}$$

where R and I are the real and imaginary components of the output, v is the rms value of the applied ac signal, R_m is the measuring resistor in the potentiostat, and where ω is the angular frequency. With our experimental configuration the best data was obtained at 80 Hz. No frequency dispersion was observed.

III. RESULTS

A. Molybdenum diselenide

Mott–Schottky plots for three $MoSe_2$(0001) crystals are shown in Fig. 2. The surfaces were prepared such that the fraction of the R surface (surface parallel to the c-lattice vector) was negligible and hence the surfaces could be regarded as atomically smooth.[18] From Fig. 2, the donor concentration (N_D) and flat band potential values were evaluated from the Mott–Schottky relationship

$$\frac{1}{C_{\text{SC}}^2} = \frac{2}{\epsilon\epsilon_0 N_D}\left(\Delta\phi_{\text{SC}} - \frac{kT}{e}\right), \tag{21}$$

assuming a value $\epsilon = 4.8$[18] (see Table I). The energy difference between the conduction band and the Fermi level in the bulk crystal was determined for each crystal by assuming complete ionization of donor atoms and applying the Maxwell–Boltzmann distribution function.

$$(E_F - E_C)_{FB} = kT \ln \frac{N_D}{N_C}, \tag{22}$$

where N_C is the effective density of conduction band states, given by

$$N_C = 2(2\pi m^* kT/h^2)^{3/2}. \tag{23}$$

A value of effective mass ($m^* = 0.5\, m_e$) and a value for the band gap ($E_g = 1.06$ eV) were taken following Kautek and Gerischer,[18] the results are shown in Table I.

For the condition of degeneracy, where the energy of the Fermi level at the surface becomes greater than the energy of the conduction band at the surface $(E_F > E_C)_s$, we see from Fig. 1 that η_s takes positive values. The space charge (Q_{SC}) in this region has been calculated for $0 < \eta < 20$, from Eq. (16), by setting η_b equal to zero for each crystal and subsequently plotting η_s with respect to their respective flat band potential values, and, for $\eta > 20$, from Eq. (18). From these values the corresponding differential capacitance values (C_{SC}) have been evaluated from Eq. (19) (see Tables II and III). For each of the $MoSe_2$ crystals C_{SC} vs $(\phi - \phi_{FB})$ has been plotted in Fig. 3. For comparison the experimental differential capacitance (C_{exp}) values are also plotted in Fig. 3. The C_{exp} values are shown to be significantly lower in the degenerate region, furthermore, at extreme negative potentials the measured values even begin to decrease.

The differential capacitance of the space charge layer (C_{SC}) approaches, in the region of degeneracy, the magnitude of the Helmholtz double layer capacitance (C_H). Therefore the contribution of C_H to the overall capacitance can no longer be neglected in the interpretation of the measured data. Since both capacitances are in series the total calculated capacitance C_T is given by

TABLE I. Band model data for n-$MoSe_2$ crystals.

n-$MoSe_2$	N_D(cm^{-3})	ϕ_{FB}/(V)	$(\phi_C - \phi_F)_{\text{FB}}$/(V)	ϕ_C/(V)	ϕ_V/(V)
A	8.6×10^{16}	−0.24	0.117	−0.36	+0.70
B	7.1×10^{17}	−0.30	0.064	−0.36	+0.69
C	1.3×10^{18}	−0.29	0.048	−0.34	+0.71

TABLE II. Calculated differential capacitance data for n-$MoSe_2$ and n-WSe_2 for $4 < (\eta_s - \eta_b) < 20$.

		n-$MoSe_2$		n-WSe_2	
η_s	$[F_{3/2}(\eta_s)]^{1/2}$	$Q_{SC}/\mu C(cm^{-2})$	$C_{SC}/\mu F(cm^{-2})$	$Q_{SC}/\mu C(cm^{-2})$	$C_{SC}/\mu F(cm^{-2})$
4.0	4.198	0.63		0.59	
5.0			6.58		6.16
6.0	6.423	0.97		0.91	
7.0			7.34		6.89
8.0	8.908	1.34		1.26	
9.0			7.95		7.44
10.0	11.59	1.74		1.63	
11.0			8.37		7.85
12.0	14.42	2.17		2.03	
13.0			8.80		8.25
14.0	17.39	2.61		2.45	
15.0			9.13		8.56
16.0	20.48	3.08		2.89	
17.0			9.43		8.86
18.0	23.67	3.56		3.34	
19.0			9.74		9.11
20.0	26.96	4.05		3.80	

TABLE III. Calculated differential capacitance data for n-$MoSe_2$ and n-WSe_2 for $(\eta_s - \eta_b) > 20$.

	n-$MoSe_2$		n-WSe_2	
$(\eta_s - \eta_b)$	$Q_{SC}/\mu C(cm^{-2})$	$C_{SC}/\mu C(cm^{-2})$	$Q_{SC}/\mu C(cm^{-2})$	$C_{SC}/\mu F(cm^{-2})$
20	4.03		3.77	
22	4.53	10.15	4.24	9.48
24	5.06		4.73	
26	5.59	10.57	5.23	9.89
28	6.13		5.73	
30	6.68	10.95	6.25	10.26
32	7.24		6.78	
34	7.81	11.31	7.31	10.58
36	8.39		7.85	
38	8.98	11.63	8.40	10.87
40	9.57		8.96	
42	10.18	11.92	9.52	11.15
44	10.78		10.09	
46	11.40	12.20	10.67	11.41
48	12.02		11.25	
50	12.65	12.45	11.84	11.65
52	13.29		12.43	
54	13.93	12.70	13.03	11.88
56	14.58		13.64	
58	15.23	12.92	14.25	12.09
60	15.89		14.87	
62	16.56	13.15	15.49	12.29
64	17.23		16.12	
66	17.90	13.35	16.75	12.49
68	18.58		17.39	
70	19.27	13.54	18.02	12.67
72	19.96		18.67	
74	20.66	13.74	19.32	12.83
76	21.36		19.98	
78	22.06	13.92	20.64	13.02
80	22.77		21.30	
82	23.48	14.09	21.97	13.18
84	24.20		22.64	
86	24.92	14.26	23.32	13.35
88	25.65		24.00	
90	26.38	14.43	24.68	13.49
92	27.12		25.37	
94	27.85	14.58	26.06	13.64
96	28.59		26.75	
98	29.35	14.73	28.15	13.79
100	30.10			

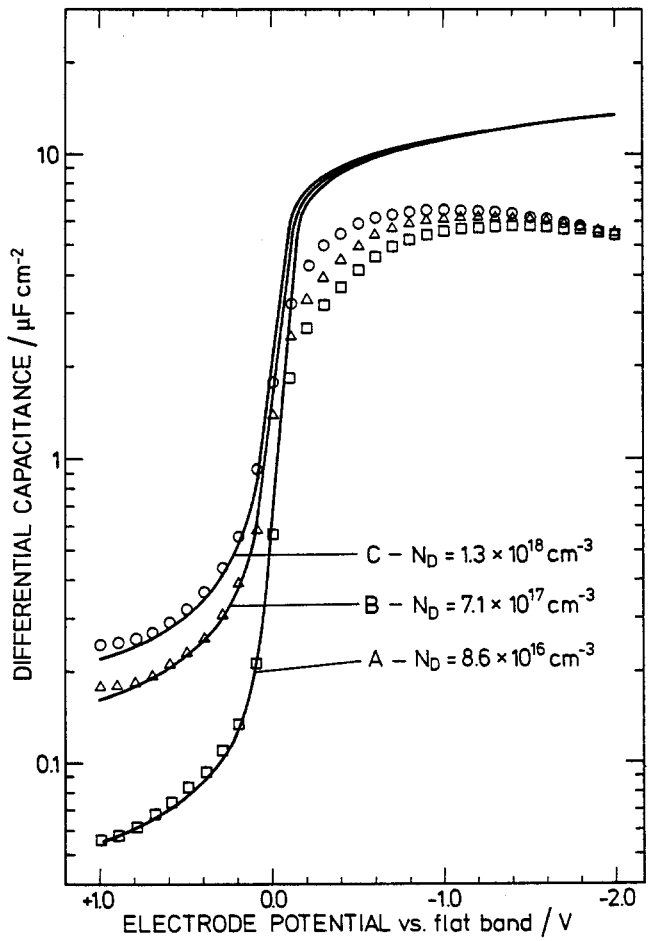

FIG. 3. Differential capacitance curves: Experimentally determined for the system n-$MoSe_2$/propylene carbonate (0.1 M $LiClO_4$), crystals A (□), B (△), and C (○). Calculated values for the n-$MoSe_2$/vacuum interface are shown as continuous curves for each of the respective crystals. The electrode potential is plotted for $U_{FB} = 0$.

$$C_T = \frac{C_{SC} \cdot C_H}{C_{SC} + C_H}. \tag{24}$$

The space charge capacitance has been calculated above in terms of the voltage drop $\Delta\phi_{SC}$. This calculation includes also the correlation between the excess negative charge in the semiconductor (Q_{SC}) and $\Delta\phi_{SC}$. However, the voltage applied experimentally ($\Delta\phi$) is larger than $\Delta\phi_{SC}$ by an amount $\Delta\phi_H$, the voltage drop in the Helmholtz layer, thus

$$\Delta\phi = \Delta\phi_{SC} + \Delta\phi_H. \tag{25}$$

For a comparison of the experimentally measured values C_{exp} and the theoretical values C_T based on Eq. (24), having already determined C_{SC}, we have now to obtain a value for C_H, taking into account the fact that C_H depends on $\Delta\phi_H$ as C_{SC} depends on $\Delta\phi_{SC}$. Fortunately, C_H has been measured in the same electrolyte, at the mercury electrode, by Hills and Reeves.[19] Assuming that the capacitance of the Helmholtz double layer has at our electrode a similar value to that for a mercury electrode, which is a reasonable assumption providing no ionic double layer exists on the small van der Waals surfaces, we can calculate the dependence of $\Delta\phi_H$ on the excess charge on the electrode and correlate these data to $\Delta\phi_{SC}$, for the same charge, in order to calculate $\Delta\phi$ from Eq. (25).

Since the differential capacitance at the mercury surface is not a constant, $Q(\Delta\phi_H)$ has to be obtained by integration from the potential of zero charge (ϕ_{pzc}), to the respective potential (ϕ),

$$Q_H(\Delta\phi_H) = \int_{\phi_{pzc}}^{\phi} C_H(\phi)\,d\phi. \tag{26}$$

$Q_H(\Delta\phi_H)$ has been calculated from Eq. (26) using the data of Hills and Reeves,[19] and is plotted together with $Q_{SC}(\Delta\phi_{SC})$ in Fig. 4. From this figure we can now determine the contribution of $\Delta\phi_H$ and $\Delta\phi_{SC}$ to the total applied potential ($\Delta\phi$) for the condition $Q = Q_H = Q_{SC}$. For convenience, C_{SC} and C_H are also plotted in Fig. 4 so that the appropriate values of $C_{SC}(\Delta\phi_{SC})$ and $C_H(\Delta\phi_H)$ may be directly obtained. From these values the total capacitance may be calculated, in analogy to Eq. (24), from

$$C_T(\Delta\phi) = \frac{C_{SC}(\Delta\phi_{SC}) \cdot C_H(\Delta\phi_H)}{C_{SC}(\Delta\phi_{SC}) + C_H(\Delta\phi_H)}. \tag{27}$$

The data for crystal C, shown in Fig. 3, are shown once again in Fig. 5, but this time the theoretical capacitance curve $C_T(\Delta\phi)$, which includes the contribution from the Helmholtz double layer, is also shown. Agreement between the experimentally measured curve and the theoretical curve $C_T(\Delta\phi)$ is shown to be reasonably good.

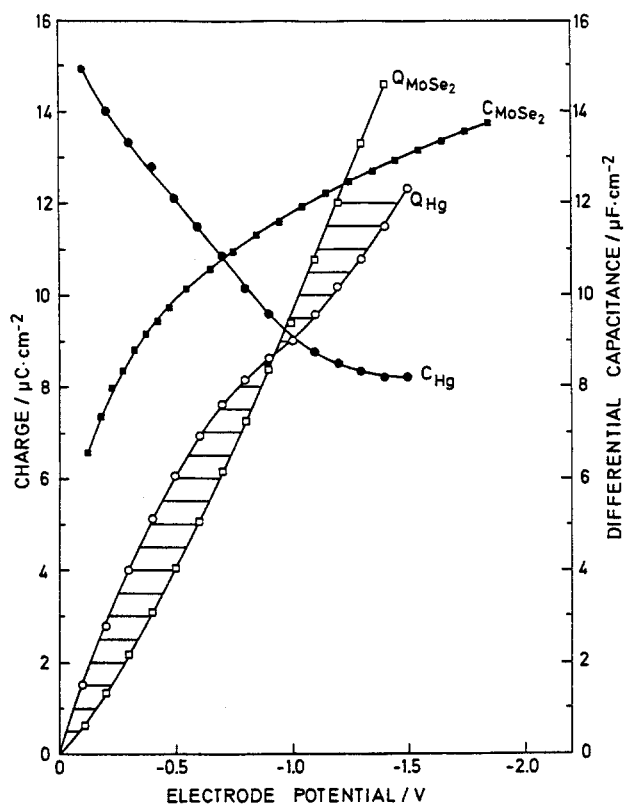

FIG. 4. Differential capacitance (C) and integral charge (Q) curves for the systems, Hg/propylene carbonate [0.1 M $Li(ClO_4)$] and n-$MoSe_2$/vacuum (crystal C). The potential scale is plotted with respect to $\phi_{pzc} = 0$ for the former and $\phi_{FB} = 0$ for the latter.

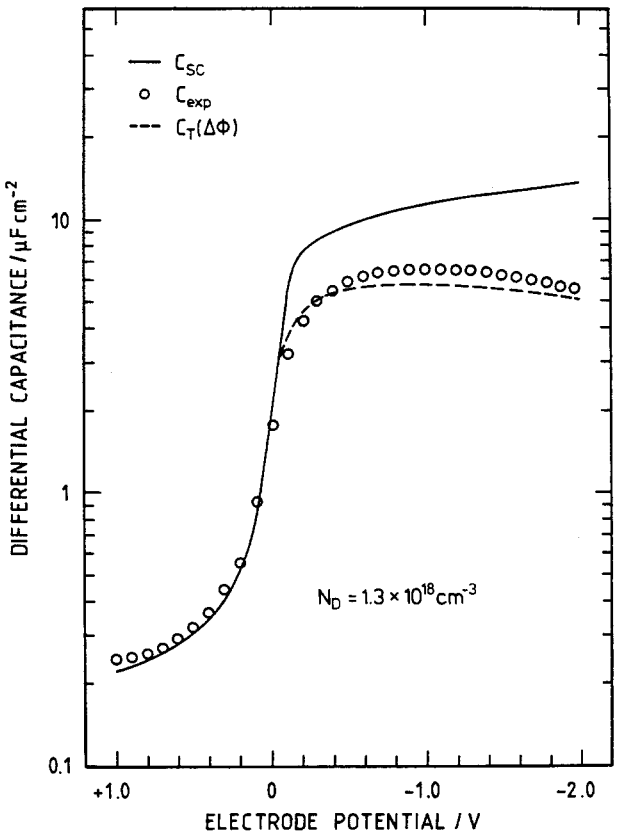

FIG. 5. Differential capacitance curves for n-$MoSe_2$ (crystal C): experimentally determined for the system n-$MoSe_2$/propylene carbonate (0.1 M $LiClO_4$) (C_{exp}); calculated for the system n-$MoSe_2$/vacuum (C_{SC}); calculated for the system n-$MoSe_2$/propylene carbonate (0.1 M $LiClO_4$) [$C_T(\Delta\phi)$]. The potential is plotted with respect to $\phi_{FB} = 0$.

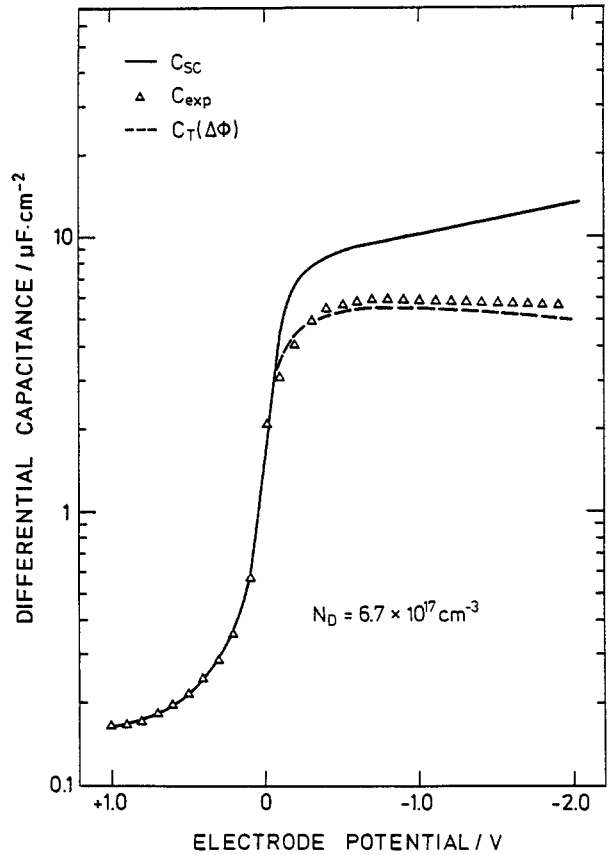

FIG. 6. Differential capacitance curves for n-WSe_2: experimentally determined for the system n-WSe_2/acetonitrile (0.1 M TPABF) (C_{exp}); calculated for the system n-WSe_2/vacuum (C_{SC}); calculated for the system n-WSe_2/acetonitrile (0.1 M TEAP), [$C_T(\Delta\phi)$]. The potential is plotted with respect to $\phi_{FB} = 0$.

B. Tungsten diselenide

For the n-WSe_2 crystal the flat band potential ($\phi_{FB} = -0.41$ V vs Ag/Ag^+) and the donor concentration ($N_D = 6.7 \times 10^{17}$ cm^{-3}) were evaluated from capacitance data, recorded in the depletion region, using Eq. (21). The potential difference between the conduction band and the Fermi level for flat band conditions [$(E_C - E_F)_{FB} = 0.065$ eV] was evaluated using Eq. (22) and Eq. (23) by assuming a value of $m^* = 0.5\, m_e$.[18]

For the condition of degeneracy $(\eta_s - \eta_b) \geqslant 0.065$ eV, the differential capacitance for the semiconductor (C_{SC}) was calculated following the procedure outlined in Sec. III A, where in this case the dielectric constant is taken to be $\epsilon = 4.2$.[18] The calculated values for both C_{SC} and the surface charge Q_{SC} are shown in Tables II and III. Figure 6 shows the curve which represents the calculated values of C_{SC} as a function of applied potential, compared with the corresponding experimentally determined values of differential capacitance (C_{exp}) for the n-WSe_2/ACN(0.2 M TPABF) interface. Once again we observe a large discrepancy between C_{SC} and C_{exp}, in the degenerate region, the latter being significantly lower than the former, with both curves diverging at more negative potentials. However, as pointed out in Sec. III A, the Helmholtz double-layer capacitance can no longer be neglected, for the interpretation of data recorded in the degenerate region.

In order to account for the Helmholtz contribution to C_{SC} we must first obtain a value for C_H, taking into account that C_H depends on $\Delta\phi_H$ as C_{SC} depends on $\Delta\phi_{SC}$. C_H has been measured by Fawcett and Loutfy[20] for the mercury electrode in ACN (0.1 M TEAP). Although, for comparison, the electrolytes should ideally be identical, both salts are tetralkylammonium salts, and since there is only a small difference between the differential capacitance curve measured in ACN containing TEA^+ and that measured in ACN containing TBA^+, at potentials negative of the pzc,[20] we anticipate that the use of the ACN (0.1 M TEAP) data is a good approximation for our own system. Using this data, $Q_H(\Delta\phi_H)$ has been calculated from Eq. (24) and is plotted together with $Q_{SC}(\Delta\phi_{SC})$ in Fig. 7. From this figure we can now determine the contribution of $\Delta\phi_H$ and $\Delta\phi_{SC}$ to the total applied potential ($\Delta\phi$) for the condition $Q = Q_H = Q_{SC}$. For convenience, C_{SC} and C_H are also plotted in Fig. 7 so that the appropriate values of $C_{SC}(\Delta\phi_{SC})$ and $C_H(\Delta\phi_H)$ can be directly determined. From these values the total capacitance, $C_T(\Delta\phi)$, may be calculated from Eq. (27). These data are introduced into Fig. 6 and can be seen to be in good agreement with the experimental data.

IV. DISCUSSION

In this section it is appropriate to address the validity of some of the approximations made in this work. First and

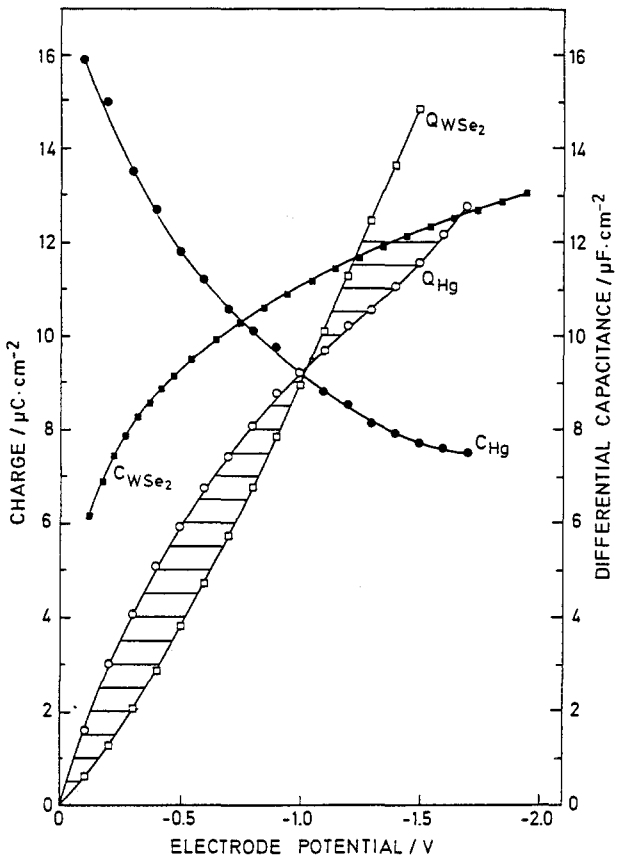

FIG. 7. Differential capacitance (C) and integral charge (Q) curves for the systems, Hg/acetonitrile (0.1 M TEAP) and n-WSe_2/vacuum. The potential is plotted with respect to $\phi_{pzc} = 0$ for the former and $\phi_{FB} = 0$ for the latter.

foremost, we have to remember that the accuracy of the experimentally determined capacitance depends strongly on whether or not the assumed RC series network is a good approximation. We can show that, for our case, where dc Faradaic currents were $< 1.0\,\mu A\ cm^{-2}$, the absolute values of the measured capacitance are accurate to well within the dimensions of the symbols used to describe the C_{exp} curves.

With respect to the calculation of the semiconductor surface capacitance: First, the assumption that the contribution of the ionized donors to the total space charge is negligible, compared to the concentration of conduction band electrons, can be quantitatively substantiated. From Eq. (6), we calculate that, for a donor concentration $\leqslant 1\times 10^{18}\ cm^{-3}$, the contribution to the total space charge is $\leqslant 1.7\%$ for values of $\eta_s - \eta_b \geqslant 5\,kT/e$. Furthermore, donors with an energy level below E_C are neutralized if E_F enters the conduction band and this decreases their contribution to Q_{SC} even more so. Second, the values used for m^* for both $MoSe_2$ and WSe_2, are bulk crystal values and as such may be unrepresentative of the density of states at the surface. However, because the capacitance is proportional $m^{*3/4}$ and because C_T is composed of two terms, C_{SC} and C_H, the former of which makes the smaller contribution, any change in the value of C_T $(\Delta\phi)$ due to a change in m^* is likely to be modest. Third, we have assumed that the experimental capacitance for the Hg/solvent interface is simply the Helmholtz capacitance. This is of course the classical assumption which considers the metal to be a perfect conductor. However, more recently, there exists a number of studies which consider the contribution of the potential dependent surface dipole of the metal to the double layer capacitance.[21–24] Experimentally there is evidence to suggest that the double layer capacity does depend on the nature of the metal[22] and attempted theoretical treatments do exist, albeit only for the potential of zero charge (pzc) as yet.[23] Similar effects could also exist in our systems but are expected to be small for potentials negative of the pzc.[24] However, at large overvoltages, C_T is mainly controlled by C_H and therefore the decrease of C_T in this range, with increasing negative bias, can only be caused by C_H since C_{SC} can only increase. This indicates that the Helmholtz capacitance, for the metal (Hg) and for these semiconductors, is indeed controlled by the same physical property and thus the decrease of C_H with ϕ_H may have, in both cases, to be attributed to dielectric saturation in the layer between the ions in solution and the solid surface, commonly referred to as the inner Helmholtz layer (IHL).

Assuming, due to dielectric saturation of the IHL, that the values of the dielectric constants for the semiconductor surface and the IHL are likely to converge with increasing negative bias; then, since C_{SC} increases and C_H decreases as the negative bias increases, the screening distance for the semiconductor surface charge must rapidly approach the dimensions of the Helmholtz layer (i.e., several angströms) as the negative bias increases. Furthermore, for the conditions of extreme degeneracy, the screening distance probably approaches values similar to that commonly expected for metal surfaces.

ACKNOWLEDGMENTS

One of us (R. M.) would like to thank Dr. W. Ekardt and Dr. J. K. Sass for their constructive criticism concerning this manuscript.

GLOSSARY OF TERMS

A	$= 4\pi(2m^*kT/h^2)^{3/2}$
B	$= Ae^2/\epsilon\epsilon_0 kT$
C_{expt}	= Experimental differential capacitance
C_H	= Helmholtz differential capacitance
C_T	= Total differential capacitance
$D_C(E)$	= Conduction band density of states function
E_C	= Conduction band energy
$b^E c$	= Bulk value of the conduction band
E_F	= Fermi energy
E_g	= Band gap energy
E_V	= Valence band energy
$f(E)$	= Fermi function
$F_j(\eta)$	= Fermi integral
m^*	= Effective mass
m_e	= Electron mass
n	= Concentration of conduction band electrons
N_D	= Density of donor states
N_C	= Effective density of conduction band states
Q_{SC}	= Semiconductor space charge
η	= Dimensionless measure of the local potential in the semiconductor

η_1 $= d\eta/dx$
η_2 $= d^2\eta/dx^2$
η_b = Bulk semiconductor value of η
η_s = Surface semiconductor value of η
ρ = Charge density
ϕ = Potential
ϕ_{FB} = Flat band potential
ϕ_H = Helmholtz potential
ϕ_{pzc} = Potential of zero charge

N.B. Where not specified all other terms have their usual meaning.

[1]W. Schottky, Z. Phys. **113**, 367 (1939); **118**, 539 (1942).
[2]N. F. Mott, Proc. R. Soc. London Ser. A **171**, 27 (1939).
[3]W. Shockley, Bell Syst. Tech. J. **28**, 435 (1949).
[4]C. G. B. Garrett and W. H. Brattain, Phys. Rev. **99**, 376 (1955).
[5]J. F. Dewald, Bell Syst. Tech. J. **39**, 615 (1960).
[6]H. Gerischer, *Advances in Electrochemical Engineering*, edited by P. Delahay (Interscience, New York, 1961), Vol. 1, p. 139, and references therein.
[7]J. McDougall and E. C. Stoner, Trans. R. Soc. London A **237**, 67 (1938).
[8]J. Gobrecht, Ph.D. thesis, Technical University, Berlin, 1979.
[9]J. A. Wilson and A. D. Yoffe, Adv. Phys. **18**, 193 (1969).
[10]A. D. Yoffe, Festkörperprobleme **8**, 1 (1973).
[11]A. D. Yoffe, Ann. Rev. Mater. Sci. **3**, 147 (1973).
[12]A. D. Yoffe, Chem. Soc. Rev. **5**, 51 (1976).
[13]J. L. Calais, Adv. Phys. **26**, 847 (1977).
[14]G. A. Tsigdinos, *Topics in Current Chemistry* (Springer, Berlin, 1978), Vol. 16, p. 56.
[15]E. Mooser, *Physics and Chemistry of Materials with Layered Structure* (Reidel, Dordrecht, 1978), Vols. 1–5.
[16]W. Kautek, H. Gerischer, and H. Tributsch, Ber. Bunsenges. Phys. Chem. **83**, 1000 (1979).
[17]O. R. Brown and R. McIntyre, Electrochim. Acta **29**, 995 (1984).
[18]W. Kautek and H. Gerischer, Ber. Bunsenges. Phys. Chem. **84**, 645 (1980).
[19]G. J. Hills and R. M. Reeves, J. Electroanal. Chem. **38**, 9 (1972).
[20]W. R. Fawcett and R. O. Loutfy, Can. J. Chem. **51**, 230 (1973).
[21]S. Trasatti, J. Electroanal. Chem. **91**, 351 (1971).
[22]S. Trasatti, J. Electroanal. Chem. **123**, 121 (1981).
[23]W. Schmickler and D. Henderson, J. Chem. Phys. **80**, 3381 (1984).
[24]F. Schulz, W. Ekardt, and J. K. Sass (to be submitted).